Int J CARS
DOI 10.1007/s11548-008-0164-2

ORIGINAL ARTICLE

Robotically assisted needle driver: evaluation of safety release, force profiles, and needle spin in a swine abdominal model

S. Shah · A. Kapoor · J. Ding · P. Guion · D. Petrisor · J. Karanian · W. F. Pritchard · D. Stoianovici · B. J. Wood · K. Cleary

Received: 10 January 2008 / Accepted: 25 April 2008

Abstract
Objective The objective of this study was to evaluate two features of a new rotating needle driver in a domestic swine model: (1) a quick release safety mechanism and (2) the impact of spinning the needle on the force proÞle.
Materials and methods The experiments were conducted in a multi-modality interventional suite. An initial CT scan was obtained to determine the location of the target, in the liver or lung. The robotic arm was positioned directly over the marked skin entry point. Control parameters were set to rotation speeds of 0, 90, or 180 rpm. The breakaway force magnitude was also preset to a predetermined force. The physician used the joystick to drive the needle towards the target while the system recorded needle insertion depth and forces.
Results Sixteen insertions were completed (14 in liver and 2 in lung) and 12 released the needle upon the desired set force. The mean response time of the quick release mechanism was 202 ± 39 ms. Needle rotation resulted in reduced insertion force.
Conclusion The robot-assisted needle insertion system was shown to be functional in a multimodality imaging clinical environment on a swine model. The system has potential future applications in precision minimally invasive procedures including biopsy and radiofrequency ablation.

Keywords Robotics/instrumentation · Safety · Minimally invasive · Rotating needle driver

The mention of commercial products, their source, or their use in connection with material reported herein is not to be construed as either an actual or implied endorsement of such products by the U.S. Food and Drug Administration, the Department of Health and Human Services or the Public Health Service.

S. Shah (✉) · A. Kapoor · P. Guion · B. J. Wood
National Institutes of Health Clinical Center,
Diagnostic Radiology Department,
Bethesda, MD, USA
e-mail: shahsap@cc.nih.gov

J. Ding · K. Cleary
Imaging Science and Information Systems (ISIS) Center,
Department of Radiology, Georgetown University,
Washington, DC, USA
e-mail: cleary@georgetown.edu

D. Petrisor · D. Stoianovici
URobotics Laboratory, Department of Urology,
Johns Hopkins Medicine, Baltimore, MD, USA

J. Karanian W. F. Pritchard
Laboratory of Cardiovascular and Interventional Therapeutics,
FDA, Laurel, MD, USA

Introduction

Minimally invasive procedures have become standard medical practice in many settings due to numerous advantages such as decreased recovery time, cost, trauma, and complications in comparison to conventional surgery. The applications of these procedures range over a variety of specialties including but not limited to urology, cardiology, neurosurgery, orthopedics, radiation oncology, oncology, and interventional radiology. Many of these minimally invasive procedures rely upon accurate insertion of a needle to an anatomical target to deliver therapy or obtain tissue samples from a pre-determined speciÞc location.

A few common examples of needle-based procedures include biopsy, radiofrequency ablation (RFA), and prostate brachytherapy. The outcome of minimally invasive procedures such as RFA depends on the size and location of the target lesion and the experience of the physician. For a complete zone of ablation, RFA requires the diameter of the ablation sphere to be 2 cm greater than the tumor to obtain a 1 cm margin [1]. Prostate brachytherapy is another needle-based procedure that requires placement of radioactive seeds at pre-planned locations around the prostate. Typically about 100 radioactive seeds are placed to provide adequate coverage of the tumor site. Currently, needles or electrodes are manually inserted into a target by the physician, primarily under image guidance. This requires a significant amount of training, coordination, and 2D to 3D extrapolation. Procedures such as these also potentially expose the patient and physician to significant radiation. Inaccuracies in needle or electrode placement for these procedures and lack of navigation devices to aid placement may result in increased procedure time, morbidity, inaccurate diagnosis, or tumor recurrence [2].

In recent years, robot-assisted needle insertion has attracted attention because of its capabilities to provide assistance in minimally invasive procedures. Computers and robots have been used in combination with these procedures and have demonstrated enhanced performance under direct physician guidance simultaneous with human input as compared to the more conventional method of the physician alone, without robotic assistance [3]. Feasibility studies have been presented by Solomon et al. [4] to develop a tumor ablation treatment system that utilizes the Acubot robot system for accurate applicator placement tested in patients. A robotically assisted needle insertion system for prostate brachytherapy has also been tested in phantoms by Fichtinger et al. [5]. The system consists of a transrectal ultrasound (TRUS) and a spatially co-registered robot. A few other robotic systems such as iGuide [6,7], Innomotion [8], Pinpoint from Philips Healthcare Inc. [9], Hata's Semi-Active robot [10], compatible with CT and MRI, are under active development by various researchers as well (see reviews [11,12] for a more exhaustive list). These systems may provide a safer working environment for the physician by limiting the amount of radiation exposure. More importantly, they are capable of enhancing outcomes by improving repeatability and accuracy which could in turn help address standardization of surgeon skill variability.

Aside from accurate placement of the needle, a major safety concern is the risk of tissue laceration due to respiratory, organ, or patient movement when using a rigid robotic needle driver. When the needle is inserted into the body, patient movement due to breathing or shift may cause laceration or trauma. Respiration can cause tissue movement of 10–20 mm or more in the area of interest [13], greatly hampering accuracy. Currently physicians try to stop patient breathing during needle insertions for up to 20–25 s time intervals [14] and advance the needle at a consistent phase of the respiratory cycle. However, this is primarily based on physician judgment and is highly variable. The problem of variability in determining a consistent phase of respiratory cycle becomes more relevant when the needle is held by a rigid device such as a robotic needle driver.

For robot-assisted needle insertion systems to be used in the clinical setting, they must overcome these safety issues. One solution is to use just a passive guide and have the physician insert the needle, as in the Neuromate [15] robotic system (Integrated Surgical Systems Inc., Davis, California, USA). At the other end of the spectrum is a fully active robotic system such as the Robodoc [16] (Integrated Surgical System Inc.) for total hip replacement. These robotic systems have addressed safety concerns, but only in clinical settings with predominantly rigid structures. Safety concerns for minimally invasive robot assisted needle insertions must take into account mobile soft tissue characteristics and dynamic tissue deformations common in non-rigid anatomy.

Tissue deformation and needle deflection are also effects which must be addressed for optimal robotic assistance. Frictional forces between the needle shaft and tissue are one of the causes of tissue deformation [17–19]. Some other factors that also affect tissue deformation include axial insertion rate and tip geometry. Force modeling has been applied to measure the stiffness, friction, and needle geometry effects during needle insertion in soft tissues [18,20]. Rotation of the needle during insertion has been explored by multiple groups [21,22] including ours, to reduce deformation and thereby decrease needle tip displacement. The effect of needle rotation during insertion has resulted in less tissue damage, indentation, and frictional forces. High-speed needle rotation in a robot assisted prostate brachytherapy system has also been shown to increase the accuracy of targeting in agar phantoms [22]. Such rotating needle driving systems may allow for more accurate needle insertions.

The aim of this paper is to evaluate the feasibility and safety capability of a new robotic-needle driving system in a swine model. The two updated mechanisms: (1) a quick release safety mechanism and (2) a rotating needle driver (RND) were evaluated by exploring the reliability of needle release and impact of spin on tissue deformation. The time to detect force overload and needle release was tested as a performance measure of the quick release safety mechanism. To test the impact of spin on tissue deformation, needle displacement and force values were compared for predetermined spin speeds. The capabilities of the robotic system demonstrated in this preclinical animal study can potentially be applied to a wide range of other needle-based, minimally invasive procedures.

Materials and methods

The robotic system used in these experiments is an updated version of the "AcuBot" system built by the Urology Robotics Laboratory at Johns Hopkins Medical Institutions [11,23]. The original AcuBot comprises the "PAKY" (Percutaneous Access of the KidneY) needle driver, the "RCM" (Remote

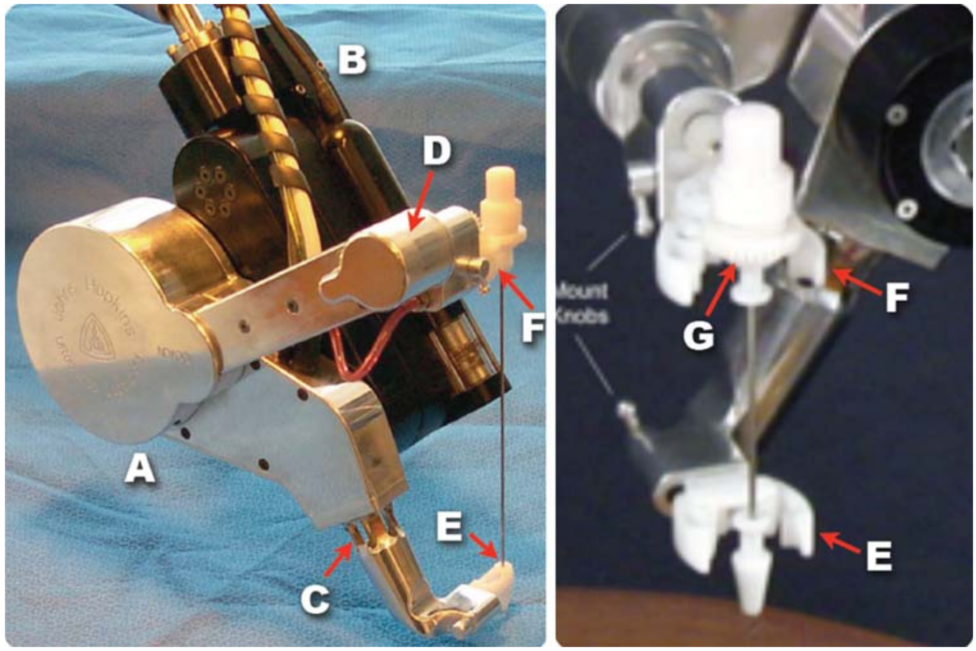

Fig. 1 *a* Rotating Needle Driver (RND), *b* Remote Center of Motion (RCM) orientation module. *c/d* Force sensor, *e/f* Head and Barrel grippers, *g* Needle hub

Center of Motion) orientation module, and joystick control. A three degree of freedom Cartesian stage, passive positioning S-arm, and Òbridge frameÓ enable the system to achieve a compact and ßexible design for interventions at multiple points along the body.

Prior experiences using the AcuBot system in clinical trials for spinal nerve blocks showed the need for some system enhancements [24]. The main focus of these enhancements was a complete redesign of the needle driver. Three new components were added to the needle driver: (1) a mechanism to spin the needle, (2) force sensors, and (3) a needle release mechanism. The updated system is referred to as the ÒAcuBot1 V2-RNDÓ and shown in Fig. 1.

The compact RND holds the needle from two points for enhanced support and accurate insertions. This design prevents buckling of long thin needles. Moreover, it is capable of spinning the needle during insertion in either direction. Rotation of the needle may help to reduce the resistive forces by the Òdrilling effect.Ó Needle rotation may also be favorable by changing a higher static friction between tissue and needle to a lower kinetic friction thus reducing insertion forces.

One unique feature of the needle driver is the built-in force sensing capability. There is a custom force sensor built into the lower arm that holds the nozzle (Fig. 1). As can be seen in Fig 2 the mechanical structure of the lower arm has been machined so that it will deßect very slightly when any force is applied to the nozzle holding the needle. Strain gages have been mounted on the lower arm to sense this deßection. Through a calibration process and calibration matrix, the output of these strain gages is converted into three orthogonal forces at the nozzle tip. Therefore, this force sensing capability measures the interaction between the needle shaft and the surrounding tissue.

The needle driver can also measure the axial force along the needle. This force is calculated by sensing the torque applied to the mechanism driving the upper arm of the needle. This torque is then converted to a force along the needle direction by accounting for the kinematics of the drive train mechanism. There is some noise from friction in this measurement, but by pressing manually along the direction of the needle and observing the reported force, it has been observed that this capability provides a reasonable representation of the actual force.

A safety mechanism is also built into the needle driver to release the needle which can be triggered manually or upon a desired force level measured by the force sensors. The needle is quickly released from the two grippers, one at the head of the needle and one close to the skin as shown in Fig. 1. The gripper at the head of the needle controls the spin and inserts the needle while the second gripper, close to the skin, guides its direction. Both grippers were fabricated from Delrin plastic and were designed to include two Þnger-like arms which clip together to hold the needle and swing aside during release as shown in Fig. 1. These grippers are low cost and can be easily manufactured to accommodate standard needle sizes. They can be sterilized and are disposable.

Experiments to test the AcuBot1 V2-RND system were performed on domestic swine in a multi-modality interventional suite, speciÞcally designed for translational and

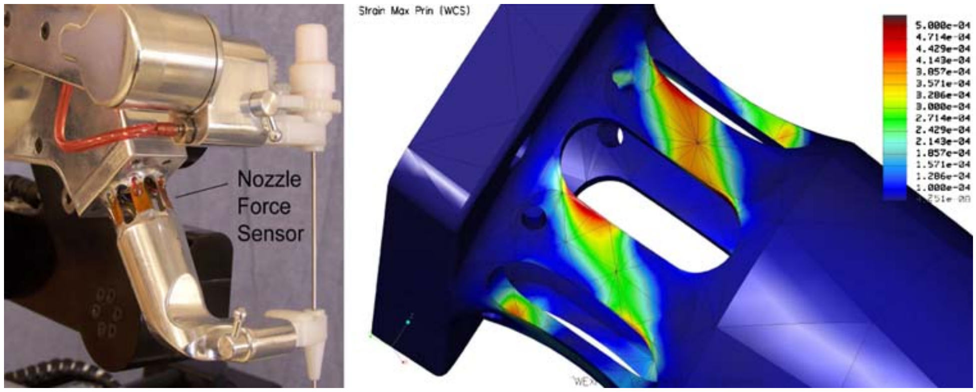

Fig. 2 Custom force sensor built into the lower arm and based on strain gage readings as shown in the right hand figure. The darker colors indicate higher strains

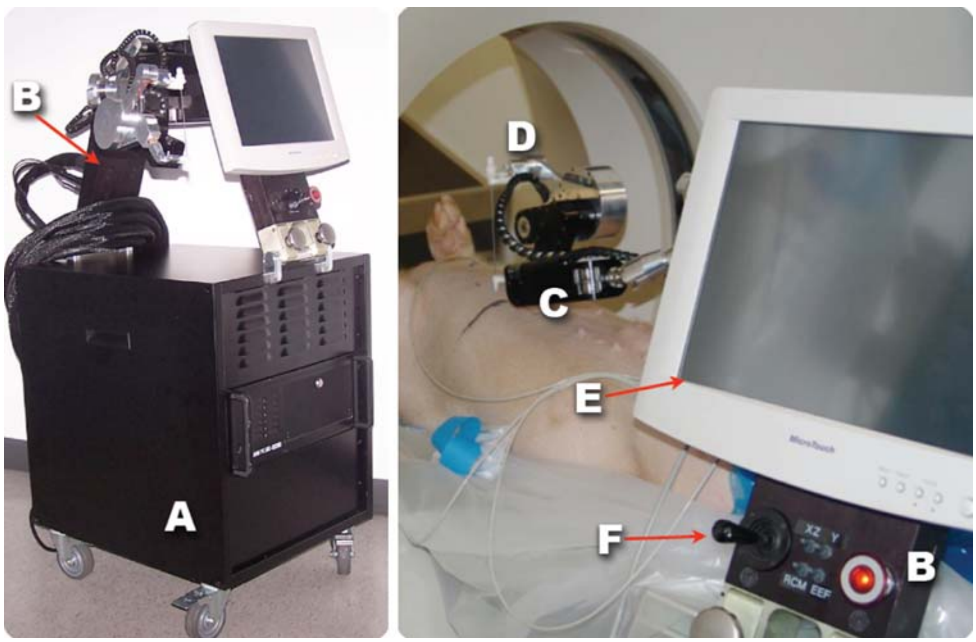

Fig. 3 *a* AcuBot1 V2-RND mounted on the control cabinet, *b* Custom “bridge frame”, *c* Needle driving unit, *d* Needle driver, *e* Computer system screen, *f* Joystick control

pre-clinical evaluation of image-guided devices. All animal care and use procedures were approved by the Institutional Animal Care and Use Committee. A domestic swine (100–125 lbs) was initially sedated with a mixture of ketamine, xylazine, telazol, and butorphanol, then intubated and maintained under general anesthesia with isoflurane. Once the animal was placed supine on the CT table, the AcuBot1 system was mounted onto the table using a custom designed mount and “bridge frame”, shown in Fig. 3a. Figure 3b shows the animal setup with the system positioned over the animal on the CT table. A preliminary CT scan was obtained to determine the location of the target in the liver. For each insertion, a different target and skin entry point were determined by the physician. The physician then marked the skin entry point on the pig. After proper securing of an 18 gauge 15 cm Diamond GREENE tip (COOK Biotech) needle within the needle driver, the robotic arm was positioned directly over the marked skin entry point.

The control parameters were then set to one of the three different rotation speeds: 0, 90, or 180 rpm. Other literature has published work with max spin values up to 2,000 rpm [25]; however, for this system the maximum spin is 180 rpm. Thus, we chose this to be our maximum rotation speed and an intermediate rotation speed of 90 rpm was also selected. At each of these speeds 6, 7, and 3 needle insertions were performed respectively. A breakaway force magnitude was also selected so that needle release would always occur due to respiratory motion. This value was enough to accommodate respiratory forces but then releasing the needle at greater forces might cause laceration. The physician also created a small incision at the marked point to facilitate needle advancement. This is not a standard practice in the clinical setting. However, due to the thickness of porcine skin compared to human skin, this was necessary to allow the needle to be inserted. The pig’s breath was held at the end of inspiration while the physician used the joystick to drive the needle towards the target.

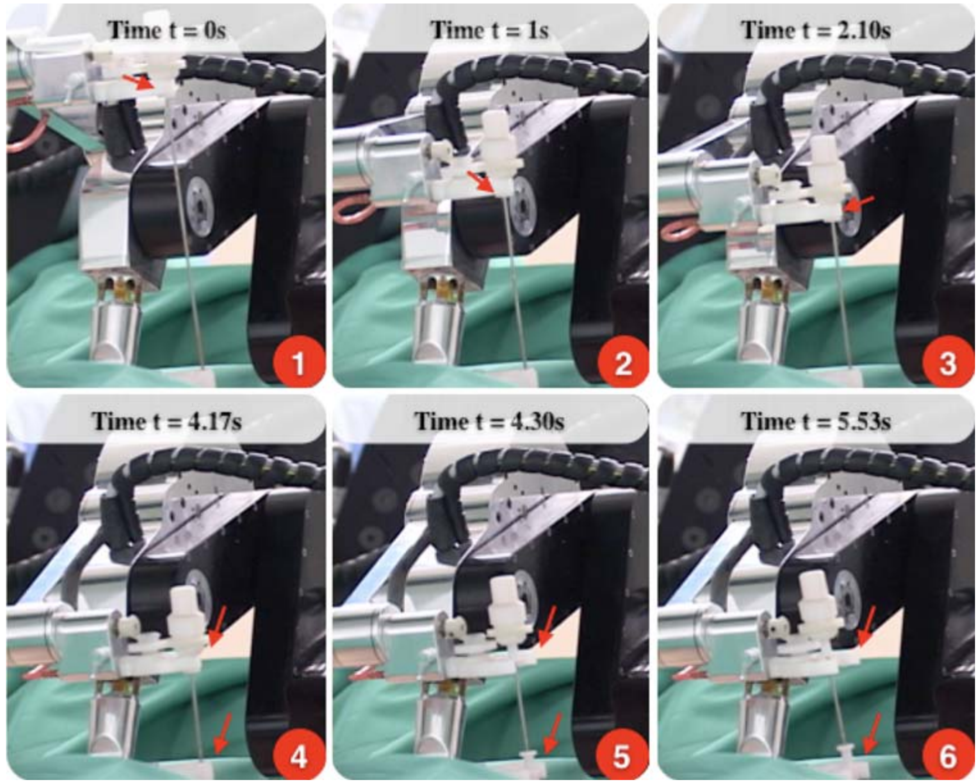

Fig. 4 A sequence of images capture the insertion of the needle using the rotating needle driver, and the subsequent smooth, quick release of the needle at the end of insertion. *1–3* display of needle insertion, *4–5* beginning and end time of needle breakaway, *6* end of needle release

The control software of the robot then recorded the needle insertion depth and forces in the X, Y, and Z directions for analysis as described later.

Figure 4 shows a typical smooth, continuous insertion of the needle and its release after reaching the target, triggered by the sensed forces. Sequences 1–3 show the needle being inserted into the pig, while sequences 4 and 5 display the beginning and end time of complete needle release from the system. Alternatively, the release could also be manually triggered by the radiologist once the insertion is completed.

Results

A total of 16 insertions, 14 in liver and 2 in lung, were performed. The two lung insertions were performed to see if there was a difference with the needle driver performance between lung and liver. There was no significant difference in the two lung trials (insertions 15 and 16 in Fig. 5b) and the liver trials. Nonetheless, of these insertions 12 released completely upon the desired set force and four failed. Two of the four failures were released before reaching proper depth during insertion and two did not release at all. Needle release prior to achieving proper depth was due to the needle interaction with more compact tissue, specifically muscle. Though the experiments were not explicitly designed to evaluate sensitivity of the force measures, these two failures suggest that the quick release mechanism should be adjusted to account for tissue variation based on CT image data. Other models to determine force profiles for this safety mechanism are being investigated. The other two failures that did not release were primarily due to excessive use and deterioration of the Delrin grippers. However, in the clinical setting, this would not be an issue because such low cost, easily manufactured parts can be disposed of after a certain number of insertions.

The response time of the quick release mechanism is also a crucial factor in ensuring safety during needle insertions. To determine the response time, we analyzed the norm of lateral forces (both x and y directions). The number of clock ticks between the controller detecting the pre-determined release threshold and the norm of the nozzle force falling below 0.1 N was recorded. The periodicity of the clock was 30 ms. Figure 5a shows a typical profile of the recorded nozzle force annotated with the start of needle release and instance when the needle is floating freely. Figure 5b displays the time between detection of a predetermined breakaway force and needle release. The mean for this measurement was 202 ± 39 ms.

A plot of the force versus needle displacement curve and average values of area under this curve with respect to needle rotation speed is shown in Fig. 6. Also shown in Fig. 6b are the maximum and minimum values for each of the spin rates.

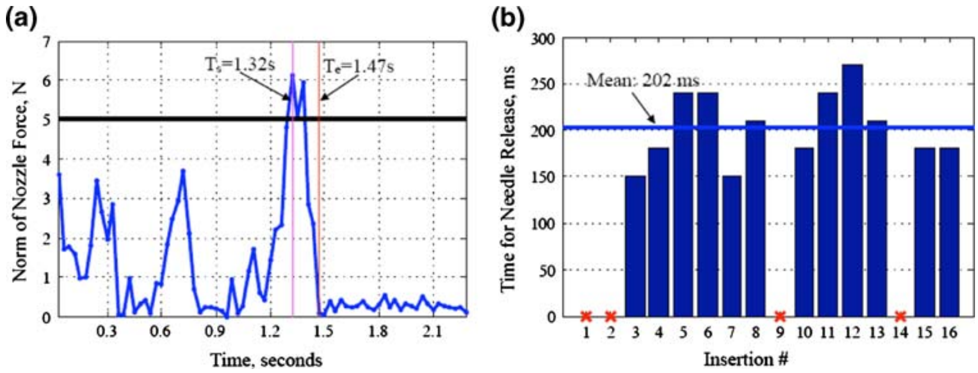

Fig. 5 **a** A typical proÞle of nozzle force recorded by the strain gauges. **b** Time between breakaway force and needle release

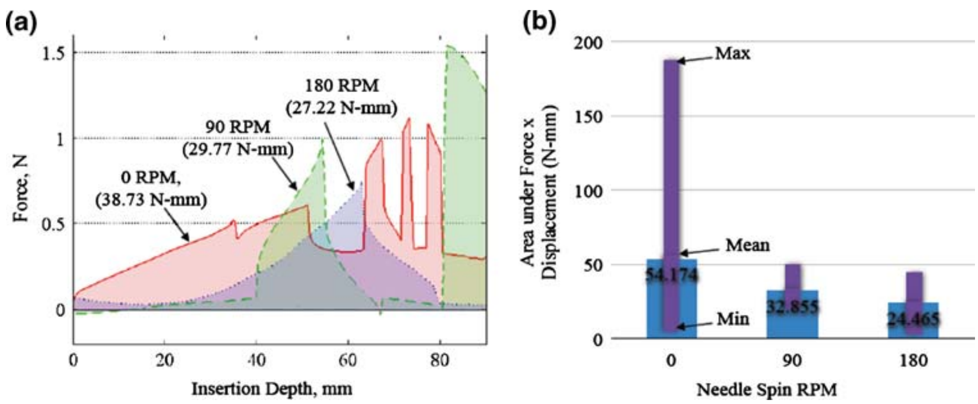

Fig. 6 **a** Force versus needle displacement curve. **b** Average areas under the Force versus Needle displacement curves of 12 successful insertions for three different spin rates. *Thin bars* represent the Range of values obtained for this metric

As seen, there is a marked reduction in the variability of this metric with rotation. This data shows the potential for needle rotation to reduce insertion force.

Discussion and conclusions

The effects of needle rotation and orientation reversal at half of the insertion depth have also been shown to increase the accuracy of targeting by other researchers [17,22]. This gain in accuracy has been shown to be due to reduced frictional forces between the needle shaft and the tissue. However, in in vivo animal models difÞculties arise when measuring the contributions obtained from needle rotation, due to factors such as respiratory motion and organ movement. The effect of needle rotation is also likely to be related to tissue type, needle beveling and tip shape. Furthermore, the inhomogenous mechanical properties of soft tissue make direct measurement of these frictional forces between the needle shaft and tissue complex and noisy as seen by the nozzle force sensor. Thus, to evaluate the effect of needle rotation we looked at the area under the force proÞle with respect to the needle insertion depth. The intuition behind this metric is that it can act as a proxy for the work done by the needle driver in inserting the needle. This measurement was collected at different points in the swine liver and values were averaged to reduce the effect of tissue inhomogeneity.

It has been suggested [21] that continuous rotation of the needle might cause more tissue damage as a result of defects in the shape of the needle. Our observations have been in line with this suggestion at high speeds, though not necessarily at lower speeds. However, our design provides two contact struts or points of support for the needle, one at the head and the second close to the skin entry point. This reduces the chance of buckling or deformation of the needle due to insertion forces.

In conclusion, a novel robotic needle driver was presented as applied to an in vivo swine model. The system was shown to be functional in a multimodality imaging clinical environment and provided a compatible workßow. The quick release safety mechanism of the system was demonstrated as a safety tool which may prevent tissue laceration and trauma, and could be a solution to a major hurdle facing active needle drivers for standard clinical practice in needle-based procedures. Safety mechanisms such as these are necessary for wider acceptance of robotic assistance in needle-based procedures. The response time for the quick release safety mechanism was sufÞcient for this proof of concept study. The RND may also provide an advantage by reducing tissue deformation and increasing the accuracy of needle targeting. Although the focus of this study was based on biopsy procedures, this robotic system can potentially be applied to a wide range of other needle-based minimally invasive procedures.

Acknowledgments Portions of this work were funded under NIH/NCI grant 5R33CA094274 and U.S. Army grant W81XWH-04-1-007, administered by the Telemedicine and Advanced Technology Research Center (TATRC), Fort Detrick, MD, USA. This research was also supported in part by the Intramural Research Program of the NIH.

References

1. Strasberg SM, Linehan D (2003) Radiofrequency ablation of liver tumors. Curr Probl Surg 40(8):459Ð498
2. Wood BJ, Locklin JK, Viswanathan A, Kruecker J, Haemmerich D, Cebral J, Sofer A, Cheng R, McCreedy E, Cleary K, McAuliffe MJ, Glossop N, Yanof J (2007) Technologies for guidance of radiofrequency ablation in the multimodality interventional suite of the future. J Vasc Interv Radiol 18:9Ð24
3. Wood BJ, Banovac F, Friedman M, Varro Z, Cleary K, Yanof J et al (2003) CT-integrated programmable robot for image-guided procedures: comparison of free-hand and robot-assisted techniques. J Vasc Interv Radiol 14:S62
4. Solomon SB, Patriciu A, Stoianovici DS (2006) Tumor ablation treatment planning coupled to robotic implementation: a feasibility study. J Vasc Interv Radiol 17(5):903Ð907
5. Fichtinger G, Fiene J, Kennedy CW, Kronreif G, Iordachita I, Song DY, Burdette EC, Kazanzides P (2007) Robotic assistance for ultrasound guided prostate brachytherapy. Med Image Comput Comput Assist Interv 10(1):119Ð127
6. Stenzel R, Lin R, Cheng P, Kronreif G, Kornfeld M, Lindisch D, Wood BJ, Viswanathan A, Cleary K (2007) Precision instrument placement using a 4-dof robot with integrated Þducials for minimally invasive interventions. In: Cleary KR, Miga MI (Eds) Proceedings of SPIE. vol. 6509, no. 1. SPIE, 2007, p 65092S. http://link.aip.org/link/?PSI/6509/65092S/1
7. Kettenbach J, Kronreif G, Figl M, FŸrst M, Birkfellner W, Hanel R, Ptacek W, Bergmann H (2005) Robot-assisted biopsy using computed tomography-guidance initial results from in vitro tests. Invest Radiol 40(4):219Ð228
8. Jantschke R, Haas T, Madoerin P, Dziergwa S (2007) Preparation, assistance and imaging protocols for robotically assisted mr and ct-based procedures. Minim Invasive Ther Allied Technol 16(4):217Ð221
9. Hevezi J, Blough M, Hoffmeyer D, Yanof JH (2002) Brachytherapy using CT PinPoint. MEDICAMUNDI 46(3):22Ð27
10. Hata N, Hashimoto R, Tokuda J, Morikawa S (2005) Needle guiding robot for mr-guided microwave thermotherapy of liver tumor using motorized remote-center-of-motion constraint. In: IEEE International Conference on Robotics and Automation, pp 1652Ð1656
11. Cleary K, Melzer A, Watson V, Kronreif G, Stoianovici D (2006) Interventional robotic systems: applications and technology state-ofthe-art. Minim Invasive Ther Allied Technol 15(2):101Ð113
12. Taylor RH (2006) A perspective on medical robotics. Proc IEEE 94(9):1652Ð1664
13. Muller SA, Maier-Hein L, Mehrabi A, Pianka F, Rietdorf U, Wolf I, Grenacher L, Richter G, Gutt CN, Schmidt J, Meinzer HP, Schmied BM (2007) Creation and establishment of a respiratory liver motion simulator for liver interventions. Med Phys 34(12):4605Ð4608
14. Riviere C, Thakral A, Iordachita II, Mitroi G, Stoianovici D (2001) Predicting respiratory motion for active canceling during percutaneous needle insertion. In: Proc 23rd Annual Intl Conf IEEE Engineering in Medicine and Biology Society, October, pp 3477Ð3480
15. Badano F, Danel F (1995) The NEURO-SKILL robot: a new approach for surgical robot development. In: MRCAS, pp 318Ð323
16. Kazanzides P, Mittelstadt BD, Musits BL, Bargar WL, Zuhars JF, Williamson B, Cain PW, Carbone EJ (1995) An integrated system for cementless hip replacement. IEEE Eng Med Biol Mag 14(3):307Ð313
17. Abolhassani N, Patel RV, Ayazi F (2007) Minimization of needle deßection in robot-assisted percutaneous therapy. Int J Med Robot 3(2):140Ð148
18. Okamura AM, Simone C, OÕLeary MD (2004) Force modeling for needle insertion into soft tissue. IEEE Trans Biomed Eng 51(10):1707Ð1716
19. Nath S, Chen Z, Yue N, Trumpore S, Peschel R (2000) Dosimetric effects of needle divergence in prostate seed implant using 125I and 103Pd radioactive seeds. Med Phys 27(5):1058Ð1066
20. DiMaio SP, Salcudean SE (2005) Needle steering and motion planning in soft tissues. IEEE Trans Biomed Eng 52(6):965Ð974
21. Abolhassani N, Patel R, Moallem M (2004) Experimental study of robotic needle insertion in soft tissue. Int Congr Ser CARSÑ Comput Assist Radiol Surg 1268:797Ð802
22. Wei Z, Ding M, Downey D, Fenster A (2005) 3D TRUS guided robot assisted prostate brachytherapy. Med Image Comput Comput Assist Interv 8(2):17Ð24
23. Stoianovici D, Cleary K, Patriciu A, Mazilu D, Stanimir A, Craciunoiu N, Watson V, Kavoussi L (2003) Acubot: a robot for radiological interventions. IEEE Trans Robot Autom 19(5):927Ð930
24. Cleary K, Watson V, Lindisch D, Taylor RH, Fichtinger G, Xu S, WC S, Donlon J, Taylor M, Patriciu A, Mazilu D, Stoianovici D (2005) Precision placement of instruments for minimally invasive procedures using a ÒNeedle DriverÓ robotÓ. Int J Med Robot 1(2):40Ð47
25. Neuenfeldt EM (2003) Method and device to reduce needle insertion force. U.S. Patent Number 6626848, Tech Rep